Articles

κM-Conotoxin RIIIK, Structural and Functional Novelty in a K^+ Channel Antagonist†

Ahmed Al-Sabi,‡ Dirk Lennartz,§ Michael Ferber,‡ Jozsef Gulyas,|| Jean E. F. Rivier,|| Baldomero M. Olivera,⊥ Teresa Carlomagno,*,§ and Heinrich Terlau*,‡

Molecular and Cellular Neuropharmacology Group, Max Planck Institute for Experimental Medicine, Hermann-Rein-Strasse 3, D-37075 Göttingen, Germany, Department of NMR Based Structural Biology, Max Planck Institute for Biophysical Chemistry, Am Fassberg 11, D-37077 Göttingen, Germany, The Clayton Foundation Laboratories for Peptide Biology, The Salk Institute, La Jolla, California 92037, and Department of Biology, University of Utah, Salt Lake City, Utah 84112

Received March 3, 2004; Revised Manuscript Received May 4, 2004

ABSTRACT: Venomous organisms have evolved a variety of structurally diverse peptide neurotoxins that target ion channels. Despite the lack of any obvious structural homology, unrelated toxins that interact with voltage-activated K^+ channels share a dyad motif composed of a lysine and a hydrophobic amino acid residue, usually a phenylalanine or a tyrosine. κM-Conotoxin RIIIK (κM-RIIIK), recently characterized from the cone snail *Conus radiatus*, blocks *Shaker* and *TSha1* K^+ channels. The functional and structural study presented here reveals that κM-conotoxin RIIIK blocks voltage-activated K^+ channels with a novel pharmacophore that does not comprise a dyad motif. Despite the quite different amino acid sequence and no overlap in the pharmacological activity, we found that the NMR solution structure of κM-RIIIK in the C-terminal half is highly similar to that of μ-conotoxin GIIIA, a specific blocker of the skeletal muscle Na^+ channel $Na_v1.4$. Alanine substitutions of all non-cysteine residues indicated that four amino acids of κM-RIIIK (Leu1, Arg10, Lys18, and Arg19) are key determinants for interaction with K^+ channels. Following the hypothesis that Leu1, the major hydrophobic amino acid determinant for binding, serves as the hydrophobic partner of a dyad motif, we investigated the effect of several mutations of Leu1 on the biological function of κM-RIIIK. Surprisingly, both the structural and mutational analysis suggested that, uniquely among well-characterized K^+ channel-targeted toxins, κM-RIIIK blocks voltage-gated K^+ channels with a pharmacophore that is *not* organized around a lysine−hydrophobic amino acid dyad motif.

Because of their diverse physiological functions in excitable and nonexcitable cells, ion channels are targets of toxins from venomous organisms, including snakes, scorpions, sea anemones, and spiders. K^+ channels are a heterogeneous group of ion channel proteins that determine and modulate a spectrum of cellular properties, including electrical excitability. Venomous organisms have evolved an amazing variety of K^+ channel-targeted polypeptide neurotoxins.

Despite the structural divergence of unrelated K^+ channel-targeted toxins, a convergent functional feature has been identified for a variety of toxins, including charybdotoxin from a scorpion, BgK from a sea anemone, and dendrotoxin from snakes. Although for the different toxins more than one site has been identified as being important for binding (for scorpion toxins, see refs *1*−*3*), all these peptides share a dyad motif of a lysine and a hydrophobic, usually aromatic, residue, which plays a key role in the interaction with the target K^+ channel (*4*−*8*). In particular, there is evidence that the lysine residue of this functional dyad occludes the K^+ channel pore (*1*−*3*). In accordance with this observation, the diverse peptides which interact with the voltage-gated K_v1 subfamily of K^+ channels (such as the *Shaker* channel from *Drosophila*) all seem to contain a functional dyad (*5*−*10*), which therefore was proposed to be a minimal functional core for the binding of the toxins to K_v1 channels.

Peptidic neurotoxins from the venomous cone snails ("conotoxins") are well-known, highly subtype-selective ligands that interact with a variety of different voltage-gated and ligand-gated ion channel targets. These cysteine-rich peptides are classified into groups based on their structural scaffolds and target specificity (*11*). κ-Conotoxin PVIIA, a *Shaker* K^+ channel blocker (*12*, *13*), was the first K^+ channel-

† This work was supported by the Biofuture Prize from the German Ministry of Education and Research (Förderkennzeichen, 0311859) (to H.T.), by the Max-Planck-Gesellschaft, and by NIH Grant GM-48677 (to B.M.O.).

* To whom correspondence should be addressed. T.C.: e-mail, taco@nmr.mpibpc.mpg.de; telephone, +49-551-201 2214; fax, +49-551-201 2202. H.T.: e-mail, hterlau@gwdg.de; telephone, +49-551-389 9474; fax, +49-551-389 9475.

‡ Max Planck Institute for Experimental Medicine.

§ Max Planck Institute for Biophysical Chemistry.

|| The Salk Institute.

⊥ University of Utah.

10.1021/bi0495681 CCC: $27.50
Published on Web 06/17/2004

```
κM-RIIIk   LOSCCSLNLRLCOVOACKRNOCCT#
μ-GIIIA     RDCCTOOKK-CKDRQCKOQRCCA#
μ-GIIIB     RDCCTOORK-CKDRRCKOMKCCA#

ψ-PIIIE    HOOCCLYGKCRRYOGCSSASCCQR#
ψ-PIIIF    GOOCCLYGSCROFOGCYNALCCRK#


κ-PVIIA    CRIONQKCFQHLDDCCSRKCNRFNKCV
```

FIGURE 1: Sequence alignment of κM-conotoxin RIIIK with other M-superfamily peptides and κ-conotoxin PVIIA. O represents 4-hydroxyproline and # an amidated C-terminal amino acid.

targeted conotoxin to be characterized. Although structurally unrelated to other known K^+ channel blockers, κ-PVIIA shares the common feature of a functional lysine−hydrophobic residue dyad (*10*). Recently, we described a novel *Conus* peptide ligand, κM-conotoxin RIIIK (κM-RIIIK), that blocks the *Shaker* K^+ channel in a state-dependent manner. By using *Shaker* channel mutants with single-residue substitutions, it was shown that κM-RIIIK interacts with the pore region of the channel. Introduction of a negative charge at residue 427 (K427D) greatly enhances the affinity of κM-RIIIK, whereas substitutions at residues F425 and T449 strongly reduced toxin affinity. The teleost homologue of *Shaker*, the trout *TSha1* K^+ channel, is the highest-affinity target of κM-RIIIK yet identified (*14*). The 24-amino acid sequence of κM-conotoxin RIIIK contains three positively charged residues but no aromatic side chain (Figure 1).

Herein, we report the solution structure of κM-RIIIK determined by NMR, together with an extensive mutational analysis of the toxin aimed at identifying the functionally relevant residues. Despite the entirely different pharmacological specificity and many differences in the amino acid sequence, we observe a striking structural similarity in the C-terminal region of κM-RIIIK and μ-conotoxin GIIIA, which specifically blocks $Na_V1.4$ Na^+ channels. The mutational analysis indicated that four amino acids (Leu1, Arg10, Lys18, and Arg19) are essential for K^+ channel binding. If κM-RIIIK contained a functional dyad, Leu1, the only hydrophobic amino acid required for activity, should be the hydrophobic part of it. However, both our structural and mutational analysis results are inconsistent with this hypothesis, clearly indicating that κM-RIIIK lacks the dyad motif found in the other K^+ channel-targeted polypeptide antagonists characterized to date. Our study on κM-RIIIK identifies a new pharmacophore for the blockade of voltage-dependent K^+ channels and provides a framework for understanding the structural determinants of the pharmacological profiles of peptide toxins interacting with voltage- and ligand-gated ion channels.

EXPERIMENTAL PROCEDURES

Peptide Synthesis.[1] Synthetic conotoxin κM-RIIIK was produced by solid phase peptide synthesis for structure determination by NMR spectroscopy. Peptides were synthesized manually on a methylbenzhydrylamine resin (2 g) (*15*) (substitution was 0.2−0.4 mequiv/g). The following side chain-protected Boc amino acids were used: Hypro(Bzl), Cys(Mob), Asn(Xan), Arg(Tos), Lys(Cl-Z), Ser(Bzl), Tyr(Br-Z), His(Tos), and Glu(Chx). Most peptide couplings were mediated for 1 h by diisopropylcarbodiimide in CH_2Cl_2 or *N*-methylpyrrolidone in the presence of HOBt and monitored by the qualitative ninhydrin test of Kaiser (*16*). Couplings including and following hydroxyproline were achieved using 3 equiv of protected amino acids (based on the original substitution of the resin) preactivated in NMP with 2.9 equiv of TBTU, 6 equiv of HOBt, and 9 equiv of DIPEA. Removal of Boc was achieved with TFA (60% in CH_2Cl_2, 1% *m*-cresol) for 10 min. After deblocking, the resin was washed with methanol followed by successive washes with triethylamine (10% in CH_2Cl_2), methanol, triethylamine, methanol, and CH_2Cl_2. The completed peptide was then cleaved from the peptido-resin (weight gain varied between 1.5 and 2.0 g) by HF containing the scavengers anisole (10%, v/v) and methyl sulfide (5%, v/v) for 90 min at 0 °C. The deprotected and cleaved peptide was precipitated in ether with 1% mercaptoethanol and separated from the spent resin by filtration after dissolution in aqueous 0.1% TFA and 60% acetonitrile. The major and desired component was isolated using preparative reverse phase HPLC using an acetonitrile gradient in a 0.1% TFA/water mixture. The fractions containing the desired peptide (300−400 mL) were combined and degassed with argon for 5 min. A buffer solution (500−600 mL) made of distilled water, 9.6 g (0.1 mol) of ammonium carbonate, 100 mg of EDTA (0.27 mmol), 250 mg of cysteine·HCl (1.6 mmol), 250 mg of cystine (1.05 mmol) and 100 mL of acetonitrile was also degassed using argon and added to the reduced peptide solution (300−400 mL); the pH (ca 8.8) was immediately adjusted to 8.2 with glacial acetic acid. The clear solution was stirred under argon for 16 h at room temperature. The folding was followed by HPLC and generally completed within a few hours.

After the folding was completed, the reaction mixture was acidified with TFA, diluted with the same volume of water, and then loaded onto a preparative HPLC (*18*) cartridge (5 cm × 30 cm) packed in the laboratory with reversed phase 300 Å Vydac C_{18} silica (particle size of 15−20 μm). The peptides eluted with a flow rate of 100 mL/min using a linear gradient of a 1% B increase per 3 min from the baseline percent of B [eluent A is 0.25 N TEAP (pH 2.25) and eluent B 60% CH_3CN and 40% A]. All peptides were subjected to a second purification step carried out with eluents A (0.1% TFA) in water and B (60% CH_3CN/40% A) on the same cartridge using a linear gradient of a 1% B increase per minute from the baseline percent of B. Analytical HPLC screening of the purified fractions was performed on a Vydac C_{18} column (0.46 cm × 25 cm, 5 μm particle size, 300 Å pore size) and a 0.1% TFA solvent system. The fractions containing the product were pooled and subjected to lyophilization. The final yield for these purified peptides was ∼5−25% (20−120 mg).

[1] The abbreviations for the common amino acids are in accordance with the recommendations of the IUPAC−IUB Joint Commission on Biochemical Nomenclature [(1984) *Eur. J. Biochem. 138*, 9−37]. The symbols represent the L-isomer except when indicated otherwise. Abbreviations: Boc, *tert*-butoxycarbonyl; Bzl, benzyl; Br-Z, 2-bromobenzyloxycarbonyl; Chx, cyclohexyl; Cl-Z, 2-chlorobenzyloxycarbonyl; CZE, capillary zone electrophoresis; DIC, *N*,*N*′-diisopropylcarbodiimide; DIPEA, diisopropylethylamine; EDTA, ethylenediaminetetraacetic acid; HOBt, 1-hydroxybenzotriazole; Hypro, hydroxyproline; Mob, 4-methoxybenzyl; NMP, *N*-methylpirrolidinone; OBzl, benzyl ester; TEA, triethylamine; TEAP 2.25, triethylammonium phosphate at pH 2.25; TBTU, 2-(1*H*-benzotriazolyl)-1,1,3,3-tetramethyluronium tetrafluoroborate; TFA, trifluoroacetic acid; Tos, tosyl; Xan, xanthydryl.

Characterization of Analogues. See the footnotes of Table 2. The purity of the final peptides was determined by analytical RP-HPLC performed with a linear gradient using 0.1 M TEAP (pH 2.5) as eluent A and a 60% CH_3CN/40% A mixture as eluent B on a Hewlett-Packard Series II 1090 liquid chromatograph connected to a Vydac C_{18} column (0.21 cm × 15 cm, 5 μm particle size, 300 Å pore size), a model 362 controller, and a Think Jet printer. Capillary zone electrophoresis (CZE) analysis was performed as described previously (*19*). Peptides are more than 90% pure as determined by HPLC and CZE in most cases. Mass spectra (MALDI-MS) were measured on an ABI-Perseptive DE-STR instrument. The instrument employs a nitrogen laser (337 nm) at a repetition rate of 20 Hz. The applied accelerating voltage was 20 kV. Spectra were recorded in the delayed extraction mode (300 ns delay). All spectra were recorded in the positive reflector mode. Spectra were sums of 100 laser shots. Matrix α-cyano-4-hydroxycinnamic acid was prepared as saturated solutions in 0.3% trifluoroacetic acid in 50% acetonitrile. The observed monoisotopic $(M + H)^+$ values of each peptide corresponded to the calculated $(M + H)^+$ values.

One-dimensional NMR spectra were used to prove the structural integrity of the alanine analogues which showed a profound reduction in the binding affinity. For these mutants (L1A, R10A, K18A, and R19A), only local chemical shift changes are observed, indicating that the overall structure is conserved.

NMR Analysis. The sample was prepared by dissolving 2.4 mg of the peptide in 300 μL of a 90% H_2O/10% D_2O mixture (pH 3.5) and the amount measured at 25 °C. A pH of 3.5 was chosen because of the lower solvent exchange rate of the H_N protons. No substantial difference was observed in the relative chemical shifts of the H_N peaks when the pH was increased to 6.5 or the temperature was reduced to 5 °C, indicating that the structure of the peptide does not vary significantly among the different conditions. An additional peptide sample for the measurement of $N-H_N$ dipolar couplings was prepared by dissolving 2.4 mg of the peptide in 14 μL of pentaethylene glycol monododecyl ether (C12E5) and 317 μL of a 10% D_2O/H_2O mixture (*19*). The nematic phase formed after addition of 2 μL of *n*-hexanol and vigorous mixing.

Resonance assignment and structural restraints were obtained by conventional NMR methods for unlabeled peptide chains (*20*). NOESY (*21*) with mixing times of 100 and 350 ms, DQF-COSY (*22*), TOCSY (*23*), and ^{15}N and ^{13}C HSQC (*24*) NMR spectra were collected on Bruker-Avance 600 and 700 MHz spectrometers.

Solvent exchange rates of the H_N protons were measured by adding 300 μL of pure D_2O to 2.4 mg of κM-conotoxin RIIIK. Eight TOCSY experiments were performed after 0, 1, 2, 4, 8, 16, 22, and 36 h. After D_2O had been added, the following H_N protons were still observable: Cys4, Ser6, Leu9, Arg10, Val14, Cys17, Lys18, Asp20, und Cys23.

$N-H_N$ residual dipolar couplings were measured in a ω_1-coupled HSQC experiment for 2.4 mg of κM-conotoxin RIIIK dissolved in the nematic phase described above.

All spectra were processed with the Bruker XWIN NMR software package (Bruker Instruments, Rheinstetten, Germany) and further analyzed with the FELIX 2000 software package (MSI, San Diego, CA). Cross-peak volumes were calculated by integration of all data points in a rectangular region, which was manually defined for each peak.

Structure Calculations. The distance restraints were classified on the basis of peak intensity in a NOESY spectrum with a mixing time of 100 ms with lower and upper bounds of 1.0−2.5 (strong), 2.5−3.5 (medium), and 3.5−5.0 Å (weak). Very weak restraints with an upper bound of 6.0 Å were obtained from the NOESY experiment with a mixing time of 350 ms. A correction of 0.5 Å was added to the upper bounds of restraints involving pseudoatoms for methyl groups. Backbone H-bonds were not included in the structure calculation.

All structure calculations were performed using an extended version of the X-PLOR 3.851 software package (*25*). The initial extended conformer was subjected to a simulated annealing protocol consisting of four steps: an initial 65 ps high-temperature phase at 2000 K followed by a first cooling phase, where the temperature was lowered to 1000 K in steps of 50 K, then by a second cooling phase, where the temperature was lowered to 100 K, and by a final energy minimization step. A total of 237 NOE-derived distance restraints were applied with soft-square potential and a force constant of 50 kcal mol^{-1} $Å^{-2}$. The stereospecific assignment of the protons of 16 methylene groups was obtained by means of a routine of the simulated annealing protocol, where the two H atoms are repetitively swapped and the configuration that best fits the experimental restraints is retained. For the remaining methylene groups, either only one resonance was observed for both protons or the experimental data were not clearly indicative of a single stereospecific assignment. Restraints involving non-stereospecifically assigned CH_2 protons were treated with the floating chirality assignment procedure of X-PLOR. A total of 17 dihedral angle restraints from $^3J(H_N,H_\alpha)$ and 12 dihedral angles restraints from $^3J(H_\alpha,H_\beta)$ coupling constants were included in the calculation.

One hundred structures were calculated, and the 13 structures with the lowest energy were used for statistics. This ensemble of 13 structures satisfied the criteria of no NOE violations of >1.0 Å and no dihedral angle violations of >5°.

Electrophysiological Measurements. The *TSha1* cDNA was kindly provided by Dr. Jeserich (University of Osnabrück, Osnabrück, Germany). *TSha1* was cloned into the psGEM vector; capped cRNA was synthesized in vitro after linearizing with Nhe1, and the transcription with T7 RNA polymerase was performed according to a standard protocol (*26*).

The oocyte expression system was used to study the effects of the wild type and the isoforms of κM-RIIIK. Oocyte preparation and RNA injection were performed as described by Jacobson et al. (*10*). Whole-cell currents were recorded under two-electrode voltage-clamp control using a Turbo-Tec amplifier (npi electronic, Tamm, Germany). The intracellular electrodes were filled with 2 M KCl and had a resistance between 0.5 and 1.2 MΩ. Current records were low-pass filtered at 1 kHz (−3 db) and sampled at 4 kHz. The bath solution was normal frog Ringer's containing 115 mM NaCl, 2.5 mM KCl, 1.8 mM $CaCl_2$, and 10 mM Hepes (pH 7.2) (NaOH). All electrophysiological experiments were performed at room temperature (19−22 °C). Toxin-contain-

ing solutions were applied by a Gilson pipet directly into the bath chamber.

The IC_{50} values of κM-RIIIK and the corresponding analogues were calculated from the reduction of whole-cell currents at a test potential of 0 mV obtained from oocytes expressing *TSha1* according to the relationship $IC_{50} = fc/(1 - fc)[Tx]$, where fc is the fractional current and [Tx] is the toxin concentration. Data are given as means ± the standard deviation. For the wild-type toxin, dose−response measurements were performed as well, resulting in an almost identical IC_{50} value (see Figure 4).

RESULTS

Structure of κM-Conotoxin RIIIK and Its Similarities to μ- and ψ-Conotoxins. The three-dimensional structure of conotoxin κM-RIIIK (Figure 2) was determined from a total of 237 NOE-derived distance restraints, 17 backbone dihedral angle restraints, and 12 side chain dihedral angle restraints. One hundred structures were generated using the simulated annealing protocol of X-PLOR (*25*), including NMR-derived structural restraints (Table 1).

κM-RIIIK is relatively flexible in aqueous solution. The rms deviation of the 13 structures with the lowest energy (Figure 2) versus the mean is 1.62 Å for the backbone atoms and 2.74 Å for all heavy atoms. The region of residues 1−11 is relatively disordered, while the C-terminal region of residues 12−24 is well-defined with a backbone rmsd of 0.78 Å. The flexibility of residues 1−11 is confirmed by the higher values of the $^1H-^{13}C$ heteronuclear NOEs of the $C_\alpha-H_\alpha$ vectors in the N-terminal part of the peptide as compared to those in the C-terminal part, as well as by the significantly reduced values of the $N-H_N$ dipolar couplings of residues 3−11. Most of the ϕ and ψ angles are in allowed regions of the Ramachandran plot, but only 37% lie in the most favored region. This indicates the presence of noncanonical or distorted structural elements, brought about by the three disulfide bridges and the four hydroxyprolines. The ω dihedral angles for all hydroxyprolines were found to be *trans* on the basis of NOEs and $^{13}C_{\beta/\gamma}$ chemical shifts.

The overall form of κM-RIIIK is that of a disk with dimensions of 15 Å × 13 Å. The three-dimensional structure of κM-RIIIK (Figure 3a, red ribbon) is very similar to that of the Na^+ channel blockers μ-conotoxins GIIIA and GIIIB (Figure 3a, blue ribbon) in the C-terminal region of residues 12−24 (*27*−*29*). The three peptides have the same disulfide connectivity, which was independently confirmed by direct chemical analysis of partially reduced intermediates of κM-RIIIK (J. Rivier, unpublished results). In the C-terminal half of the peptide, a γ-turn between Cys12 to Val14 is followed by a short distorted right-handed helix between Hyp15 and Lys18. The tail of the peptide contains a final 3_{10}-helix turn between Asn20 and Cys23. The presence of these structural elements is confirmed by the slowed solvent exchange kinetics of the amide protons of Val14, Cys17, Lys18, Asn20, and Cys23. On the other hand, the structure of κM-RIIIK significantly differs from that of μ-GIIIA in residues 1−11. The N-terminal region of μ-GIIIA consists of very tight turns (residues 2−5 and 5−8) which position the N-terminal tail in the opposite direction with respect to the C-terminus (Figure 3b). Conversely, the N-terminal region of κM-RIIIK consists of an extended tail terminated by Cys4 followed by a wide loop between Cys5 and Leu11. In conotoxin κM-RIIIK, the N-terminal tail protrudes into solution almost perpendicular to the flat surface of the peptide and to the C-terminal end (Figure 3b).

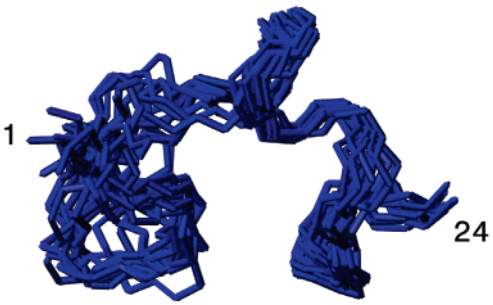

FIGURE 2: Superimposition of the 13 lowest-energy structures of κM-conotoxin RIIIK. Residues 1−11 have a high degree of flexibility, while residues 12−24 are well-defined.

Table 1: Structural Statistics[a] of the κM-RIIIK Peptide

restraints for calculation	
total no. of NOE restraints	237
intraresidue	155
sequential	51
long-range	31
dihedral angle	29
restraint violations (mean and standard deviation)	
distance restraints of ≥0.3 Å[b]	0.20 ± 0.02[b]
dihedral angle restraints of ≥5.0°	0.02 ± 0.02
coupling constant restraints of ≥0.5 Hz	0.24 ± 0.1
deviation from idealized geometry	
bonds (Å)	0.002
angles (deg)	0.48
dihedrals (deg)	1.73
energies (kcal/mol)	
restraint energy	19 ± 6
total energy	52 ± 7
Ramachandran statistics (%)	
most favored	37.2
additionally allowed	55.8
generously allowed	5.8
disallowed	1.3
rms deviation from mean structure (Å)	
backbone atoms	1.62
all heavy atoms	2.74

[a] Structure statistics refers to an ensemble of 13 structures with the lowest energy from 100 calculated structures. [b] No distance restraint was violated by more than 1.0 Å.

Recently, the three-dimensional structures of two ψ-conotoxins, ψ-PIIIE and ψ-PIIIF, antagonists of the nicotinic acetylcholine receptor, have been determined in solution by NMR (Figure 3a,b, green ribbon) (*30*, *31*). The disulfide bond pattern of these small peptides is homologous to that of both κM-RIIIK and μ-GIIIA, although their natural receptor belongs to a different superfamily, the ligand-gated ion channels. The fold of the C-terminal part of ψ-PIIIF is similar to that observed for both κM-RIIIK and μ-GIIIA, with two helical turns involving the last three cysteine residues. However, the N-terminal part of ψ-PIIIF, which consists of well-defined β-turns, differs in structure from both κM-RIIIK and μ-GIIIA. The series of β-turns, which structurally differentiate the N-terminus of ψ-PIIIF from the wide flexible loop of κM-RIIIK, place the N-terminal tail perpendicular to the flat surface of the peptide (Figure 3b), similar to the case in κM-RIIIK but unlike that in μ-GIIIA. Although well-defined turns are situated in homologous positions in μ-GIIIA and ψ-PIIIF, the geometry of these turns is not the same,

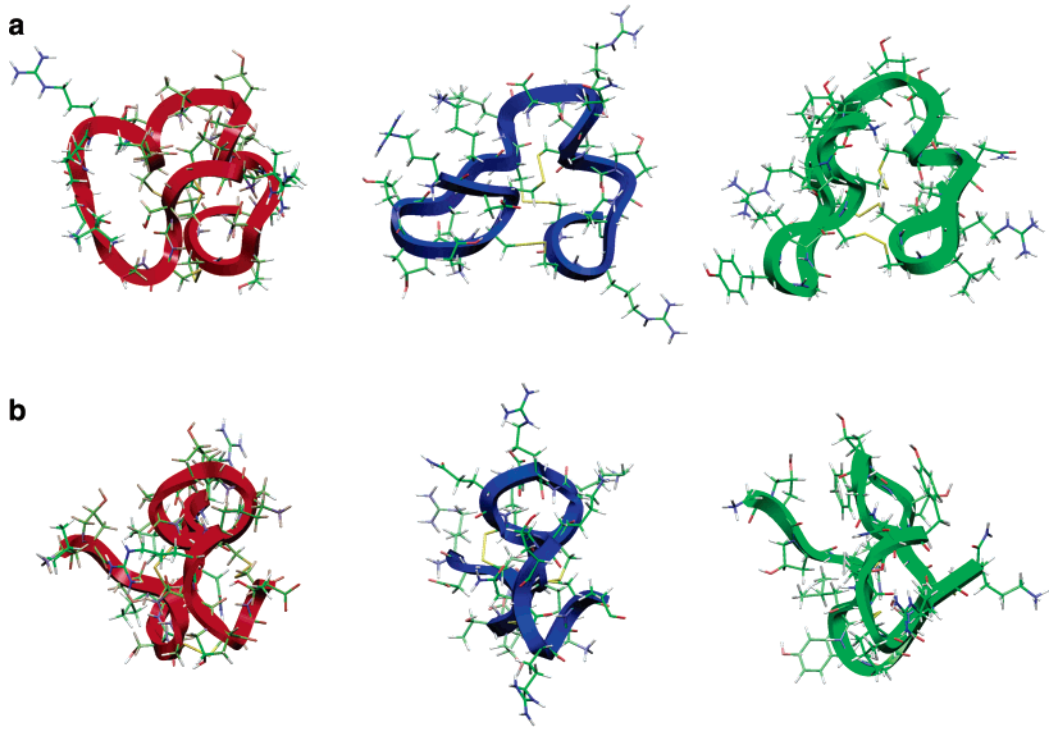

FIGURE 3: (a) Comparison of the structures of κM-conotoxin RIIIK (red ribbon), μ-contoxin GIIIA (blue ribbon; PDB entry 1TCG), and ψ-conotoxin PIIIF (green ribbon; PDB entry 1JLP). The N-terminus is on the left side and the C-terminus on the right side for each peptide. The structure of the three peptides is very similar in the C-terminal part, while the N-terminal part shows conspicuous differences. (b) Same as panel a after a rotation of 90°. This orientation was chosen to highlight the different position of the N-terminal tail in the three peptides.

bringing about the difference in the positioning of the N-terminus in the two toxins. Furthermore, unlike conotoxins κM-RIIIK and μ-GIIIA, ψ-PIIIF has the form of a lens rather than a disk (Figure 3b).

The cysteine bridges in the three peptides exhibit substantial differences in conformational flexibility. The two Cys bridges, Cys4−Cys17 and Cys5−Cys22, are quite disordered in κM-RIIIK and average between an *R* and an *S* conformation, probably as a consequence of the mobility of the loop of residues 5−11 ($\chi_2 = -60°$ for all Cys residues). Conversely, the corresponding cysteine bridges in μ-GIIIA and ψ-PIIIF are well-defined. The Cys12−Cys23 disulfide bridge of κM-RIIIK deserves a particular comment. The H_β resonances of Cys12 are degenerate, and the H_N signal is extremely weak, which indicates the possibility of conformational averaging on a millisecond time scale. Such resonance broadening had been observed before for the corresponding Cys10 of μ-GIIIA and μ-GIIIB. The observation that the H_N resonance of Cys10 is sharpened at lower temperatures motivated the structural analysis of μ-GIIIA and μ-GIIIB at 10 °C (*27*−*29*); in contrast, we do not observe any sharpening of the H_N resonance of Cys12 when the temperature is decreased from 25 to 5 °C. In κM-RIIIK, the Cys12−Cys23 bridge shows conformational averaging between an *R* and an *S* conformation ($\chi_1 = -60°$ for Cys23; the χ_1 of Cys12 cannot be determined due to the degeneracy of the H_β protons), which is similar to the case for the corresponding disulfide bridge in ψ-PIIIF (*30*). Conversely, in μ-GIIIA the Cys10−Cys21 bridge assumes only one well-defined conformation at 10 °C, despite the observed broadening of the H_N resonance of Cys10 at 25 °C. The flexibility of the Cys12−Cys23 disulfide bridge and its homologues in ψ-PIIIF and μ-GIIIA at room temperature is potentially mechanistically important, as it would allow for conformational changes upon binding to the receptor.

The three conotoxins κM-RIIIK, μ-GIIIA, and ψ-PIIIF share a common cysteine bridge pattern and a similar folding of the C-terminal part of the polypeptide chain, despite the large diversity in the receptor specificity. We speculate that the structural difference at the N-terminus of the polypeptide chain, the degree of conformational flexibility, and the different charge distribution in the three-dimensional space are key determinants of the target selectivity of these peptides.

Conotoxin κM-RIIIK is structurally unrelated to conotoxin κ-PVIIA, despite the fact that the two peptides have overlapping binding sites within the pore region of the *Shaker* K^+ channel, as indicated by the loss of activity upon mutations of F425 and T449 for both conotoxins κM-RIIIK and κ-PVIIA (*13*, *14*). The secondary structure elements are very different, with the three-dimensional structure of conotoxin κ-PVIIA mainly consisting of two large loops stabilized by a triple-stranded β-sheet. A weak similarity can be recognized in the overall shape, which resembles a disk for both peptides. Moreover, as in conotoxin κM-RIIIK, extensive flexibility was found for two of the three disulfide bridges of conotoxin PVIIA.

Identification of the Residues that Are Important for Binding. We synthesized analogues of κM-RIIIK containing alanine substitutions at each amino acid position except for the cysteine's. All analogues were synthesized manually on a methylbenzhydrylamine resin using the Boc strategy; they were cleaved in HF to yield the fully deprotected reduced peptides. After an initial RP-HPLC purification step using a 0.1% TFA in water/acetonitrile gradient, the peptides were oxidized/folded using the cystein/cystein red-ox system.

Table 2: Chromatographic and Mass Spectrometric Characterization of Peptides

κM-RIIIK	HPLC[a]	CZE[b]	MS calcd[c]	MS found[d]
wild type	98	91	2648.16	2647.9
L1A	100	98	2606.12	2606.2
O2A	98	99	2606.15	2606.1
S3A	100	98	2632.17	2632.3
S6A	97	99	2632.17	2632.1
L7A	97	99	2606.12	2606.2
N8A	80	90	2605.16	2605.1
L9A	98	96	2606.12	2606.3
R10A	80	95	2563.10	2563.3
L11A	93	88	2606.12	2606.3
O13A	100	99	2606.15	2606.1
V14A	93	98	2620.13	2620.1
O15A	98	98	2606.15	2606.2
K18A	94	98	2591.10	2590.9
R19A	98	99	2563.11	2563.0
K18R/R19K	98	97	2648.16	2648.0
N20A	87	99	2605.16	2605.2
O21A	97	95	2606.15	2606.1
T24A	98	97	2618.15	2618.1
Ac-L1	94	96	2690.17	2690.0
L1E	98	95	2663.11	2664.2
L1H	100	99	2672.14	2672.3
L1I	100	96	2648.16	2648.3
L1M	100	96	2666.12	2666.1
L1K	98	96	2663.17	2663.0
L1R	99	99	2691.17	2691.2
L1F	99	99	2682.15	2682.3
L1Y	99	99	2698.14	2698.0

[a] The percent purity was determined by the HPLC using buffer system: A being TEAP (pH 2.5) and B being 60% CH_3CN and 40% A with a gradient slope of 1% B/min, at a flow rate of 0.2 mL/min on a Vydac C18 column (0.21 cm × 15 cm, 5 μm particle size, 300 Å pore size). Detection was at 214 nm. [b] Capillary zone electrophoresis (CZE) was carried out using a Beckman P/ACE System 2050 controlled by an IBM Personal System/2 Model 50Z and using a ChromJet integrator. The field strength was 15 kV at 30 °C, with a mobile phase of 100 mM sodium phosphate (85:15 H_2O/CH_3CN mixture) at pH 2.50, on a Supelco P175 capillary column (363 μm outside diameter × 75 μm inside diameter × 50 cm length). Detection was at 214 nm. [c] The calculated $[M + H]^+$ monoisotopic masses. [d] The observed $[M + H]^+$ monoisotopic masses.

Under these conditions, peptides folded within a few hours to give a single isomer in excellent yields. Oxidized peptides were purified using preparative RP-HPLC in at least two different solvent systems (0.25 N TEAP at pH 2.25 and 0.1% TFA on C18 silica) and characterized as shown in Table 2 using RP-HPLC, CZE, and mass spectrometry as described previously (*32*).

The affinity of the alanine isoforms was functionally assayed by two-electrode voltage clamp measurements using *Xenopus* oocytes expressing the trout *TSha1* K^+ channel, the cloned K^+ channel isoform with the highest affinity for κM-conotoxin RIIIK ($IC_{50} \approx 70$ nM) identified so far, which is reversibly blocked by the toxin (see Figure 4). The results of these assays are shown in Table 3.

For six amino acids (O2, S6, L7, L9, O21, and T24), the alanine substitution resulted in an IC_{50} value that was within 5-fold of that of wild-type κM-RIIIK. We note that some substitutions (O2A, S6A, and L7A) cause a larger change in the IC_{50} value than others (L9A, O21A, and T24A), indicating that although these residues are not dominant determinants for binding they may slightly contribute to the interaction with the *TSha1* channel.

Alanine mutations of seven (S3, N8, L11, O13, V14, O15, and N20) residues exhibited an intermediate behavior, with

Table 3: IC_{50} Values for *TSha1* K^+ Block of κM-RIIIK and Analogues

κM-RIIIK	$IC_{50} \pm$ SD	*n*	$IC_{50mutant}/IC_{50WT}$
wild type	73 ± 34	7	1
L1A	3180 ± 300	6	44
O2A	210 ± 40	3	3
S3A	760 ± 280	6	10
S6A	240 ± 80	3	3
L7A	310 ± 100	6	4
N8A	420 ± 140	3	6
L9A	90 ± 20	3	1
R10A	4220 ± 860	7	58
L11A	970 ± 300	6	13
O13A	510 ± 170	6	7
V14A	1130 ± 390	5	15
O15A	850 ± 180	3	12
K18A	3920 ± 1300	6	54
R19A	1530 ± 710	9	21
K18R/R19K	180 ± 100	7	2
N20A	430 ± 70	3	6
O21A	130 ± 30	3	2
T24A	120 ± 50	3	2

IC_{50} values more than 5-fold greater but less than 16-fold than that of wild-type IC_{50}. Interestingly, S3, L11, O13, V14, O15, and N20 are located on the same side of the molecule.

Figure 5 shows that mutations of four other residues (L1, R10, K18, and R19) resulted in a major reduction of the affinity for *TSha1* K^+ channels (Table 3). The IC_{50} values of these analogues are increased by more than 20-fold, indicating an important role of these amino acids in receptor binding. Interestingly, the affinity of the double mutant K18R/R19K for the *TSha1* K^+ channel is close to that of the wild type, indicating that the positive charge is important at both positions, but the specific nature of the side chain is not critical for the interaction with the *TSha1* K^+ channel. Somewhat surprisingly for a peptide blocking K^+ channels, these four critical residues are distributed at various sites in the molecule (Figure 6a). Furthermore, the structure of κM-RIIIK does not provide any evidence of the existence of a hydrophobic−positively charged amino acid dyad, as Leu1, the most important hydrophobic residue for binding, is more than 6 Å from any positive charge.

Evaluation of Additional Substitution Mutations at Leu1. The alanine walk identified Leu1 as the only hydrophobic residue that substantively affects binding of κM-conotoxin RIIIK to the *TSha1* channel. The solution structure determined by NMR indicates that Leu1 is too far from any positively charged residue to serve as the hydrophobic component of a dyad, a conserved motif in otherwise divergent K^+ channel-targeted toxins. However, the fact that the N-terminal region (amino acids 1−11) is flexible leads to some reservations regarding this conclusion. In other toxins, the hydrophobic component of the dyad is most commonly an aromatic residue, while a lysine plays the role of the positively charged component; this lysine occludes the extracellular opening of the ion channel pore. Thus, if Leu1 is part of a functional dyad that forms following a conformational change upon binding of the receptor, it is reasonable to predict that the substitution of the leucine with an aromatic amino acid can be well-tolerated and perhaps even leads to an increase in binding affinity. To test this hypothesis, we evaluated the effect of various substitutions of Leu1 on the interaction of κM-RIIIK with the *TSha1* channel (Table 4).

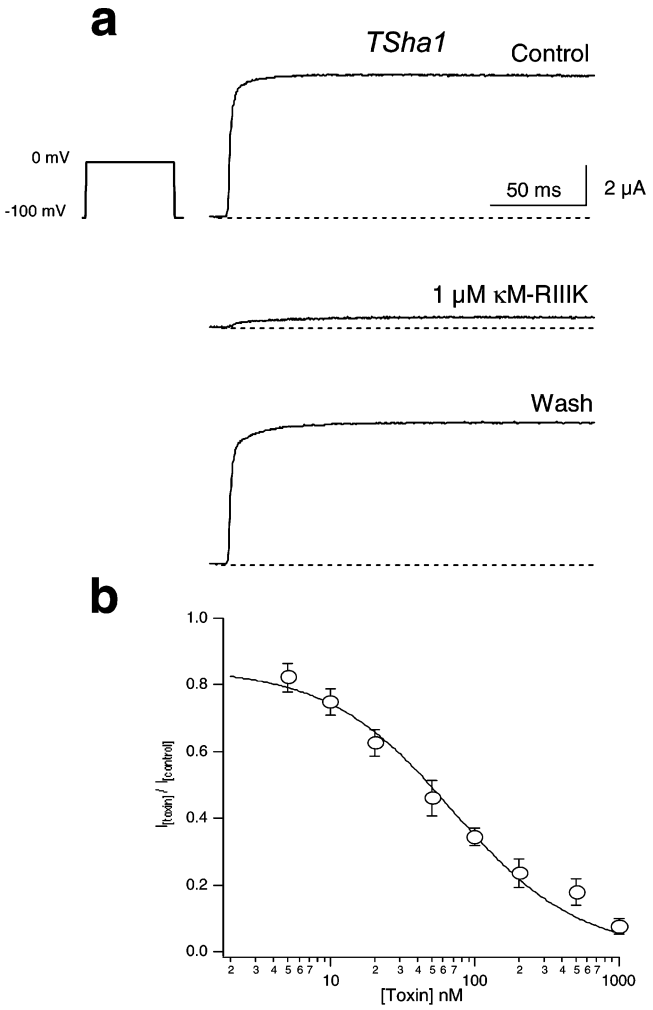

FIGURE 4: κM-Conotoxin RIIIK reversibly blocks *TSha1*-mediated currents. (a) Whole-cell currents recorded from oocytes expressing *TSha1* K^+ channels upon depolarization to 0 mV are shown before (control), after addition of 1 μM κ-conotoxin RIIIK, and after subsequent wash with NFR, indicating the reversibility of the block of the toxin. The holding potential was −100 mV. (b) Dose−response curve for the block of *TSha1* current by κM-RIIIK at a test potential of 0 mV (total number of experiments = 12 with *n* between 4 and 11 for the different indicated toxin concentrations). The IC_{50} from these measurements is 70 ± 11 nM which is almost identical to the value from the measurements of the fractional currents (see Table 2). The Hill coefficient was close to 1.

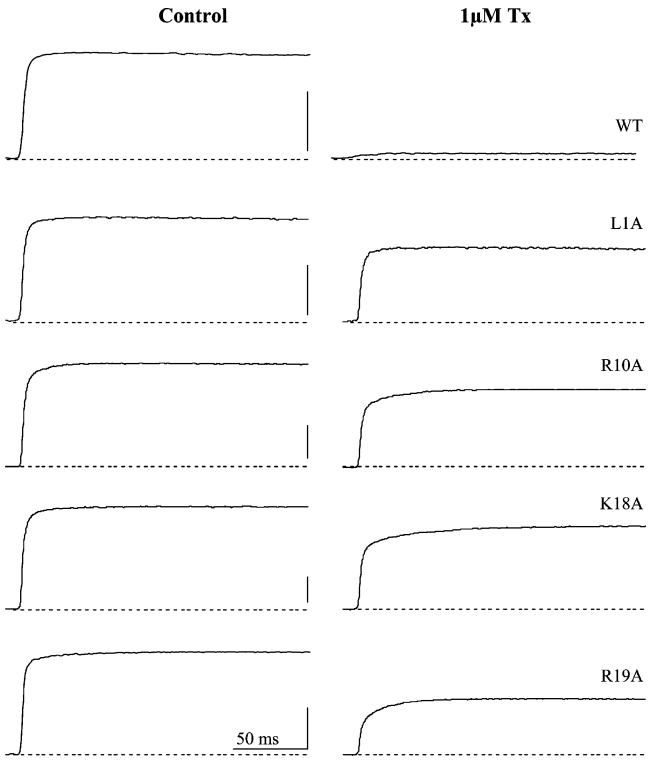

FIGURE 5: Mutation of residues L1, R10, K18, and R19 results in isoforms of κM-conotoxin RIIIK with low affinity for *TSha1* channels. Whole-cell currents recorded from oocytes expressing *TSha1* K^+ channels before and after addition of the κM-RIIIK isoform are shown. Notice the apparent slowing of activation of the currents in the presence of R10A, K18A, and R19A illustrating the re-equilibrium of toxin binding to the open state (*14*). The pulse protocol was like that described in the legend of Figure 4. The vertical bars represent 2 μA.

In contrast to what was predicted on the basis of the dyad hypothesis, both a phenylalanine (the most common amino acid as the hydrophobic half of the dyad) and a tyrosine substitution for Leu1 caused a greater apparent decrease in affinity (>100-fold) than the L1A substitution (~40-fold). Unexpectedly, the replacement of Leu with a positively charged amino acid (e.g., the L1R and L1K mutations) had a weaker effect on the affinity for the *TSha1* channel (3- and 13-fold, respectively) than the L1A mutant. Introducing a negative charge (L1E) or blocking the positive charge (N-acetylated κM-RIIIK) causes a drastic decrease in affinity (>500- and >100-fold, respectively).

The data in Tables 3 and 4 do not support the involvement of Leu1 in a dyad. This result, together with the structural data that indicate that Leu1 is not close to any positively charged side chain, allows us to conclude that this leucine does not serve as the hydrophobic component of a dyad.

DISCUSSION

We have presented the structural and mutational analysis of κM-conotoxin RIIIK, the smallest known conotoxin targeted to the K_v1 subfamily of voltage-gated K^+ channels, with the aim of defining a pharmacophore model for the interaction of this toxin with the *TSha1* channel. The solution conformation of κM-conotoxin RIIIK differs substantially from that of κ-conotoxin PVIIA, the only other structurally characterized conotoxin that interacts with the K^+ channels. While the two conotoxins share common binding sites on the *Shaker* K^+ channel, they dramatically differ in the disulfide bond pattern, secondary structure elements, and charge distribution. κM-Conotoxin RIIIK is encoded by a gene belonging to the M-superfamily, while κ-PVIIA belongs to the O-superfamily. The latter superfamily includes ω-conotoxins, which are targeted to voltage-gated Ca^{2+} channels. The most well-characterized member of the M-superfamily is μ-conotoxin GIIIA, an extremely specific blocker of the $Na_v1.4$ voltage-gated Na^+ channel subtype. The structure of κM-RIIIK is much more similar to that of μ-GIIIA than to that of κ-PVIIA. Clearly, the shared class III Cys pattern of κM-RIIIK and μ-GIIIA is the dominant determinant of the overall structure. Despite the structural similarity, κM-RIIIK and μ-GIIIA show no overlap in pharmacological specificity at all.

The structural divergences between κM-RIIIK and κ-PVIIA pose the intriguing question of whether the mechanism of the K^+ channel conductance block of the

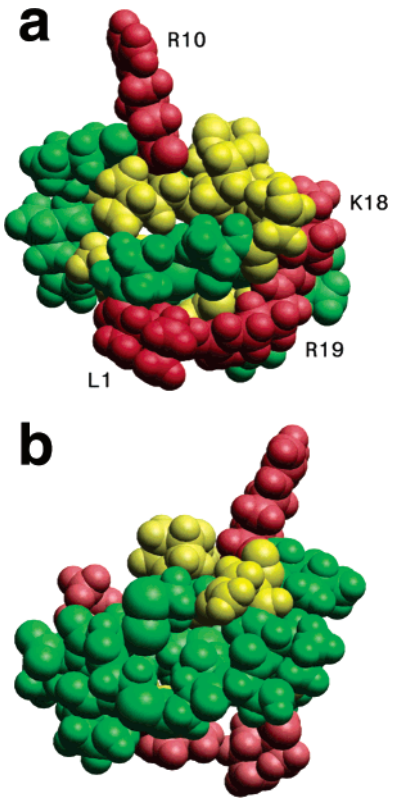

FIGURE 6: (a) Map of the functionally important residues of κM-conotoxin RIIIK on the three-dimensional structure. To visualize the different changes in the affinity observed for the corresponding alanine mutants, the residues are color-coded: red for an alanine substitution that increased the IC_{50} of κM-RIIIK by more than 20-fold (L1, R10, K18, and R19), yellow for an alanine substitution that affected the affinity by more than 5-fold but by less than 16-fold (S3, N8, L11, O13, V14, O15, and N20), and green for the rest. (b) Same as panel a but from the opposite side.

Table 4: Mutations of L1 Affect the Affinity of κM-RIIIK for the *TSha1* K^+ Channel

κM-RIIIK	$IC_{50} \pm SD$	*n*	$IC_{50mutant}/IC_{50WT}$
wild type	73 ± 34	7	1
L1A	3180 ± 300	6	44
Ac-L1	7630 ± 760	6	104
L1E	56500 ± 27670	5	774
L1H	5430 ± 790	4	74
L1I	1380 ± 1000	5	19
L1M	340 ± 110	5	5
L1K	950 ± 270	4	13
L1R	190 ± 10	3	3
L1F	5260 ± 1420	4	72
L1Y	12300 ± 1920	3	168

two toxins significantly differs. Despite their differences in size, amino acid sequence, structure, and biological origin, all other well-characterized toxins (e.g., dendrotoxin from snakes and various scorpion and sea anemone toxins), including κ-PVIIA, share a number of convergent features. The key amino acid determinants for the interaction with the K^+ channel are localized on one side of the toxin surface, and the pharmacophore is based on a hydrophobic−positively charged amino acid dyad motif. Encouraged by the similarity in the mechanisms of interaction with the K^+ channels of structurally and phylogenetically different peptides, we had expected κM-conotoxin RIIIK to fit in the common framework and to interact with K^+ channels with a dyad-based pharmacophore.

Conversely, the structural and mutational analyses described above indicate that κM-RIIIK does not fit the established paradigm. κM-RIIIK is a relatively flat disk-shaped molecule in which important amino acid determinants for binding are not clustered on the toxin surface into a clearly defined pharmacophore (Figure 6). Most importantly, κM-RIIIK does not appear to have a dyad motif composed of a hydrophobic amino acid and a lysine residue. Our conclusion that a dyad does not exist is based on two types of experimental data. First, the structure shows no hydrophobic residue within 6 Å of a positively charged residue. Second, we found that substitutions of aromatic residues for Leu1, the functionally most important hydrophobic amino acid in κM-RIIIK, are tolerated even less than Ala. Furthermore (and most unexpectedly), substitution of a positive charged amino acid gave an affinity close to that of the wild-type peptide. In fact, the Leu1 substitution with the smallest effect on the affinity of the peptide is an arginine (L1R) and not isoleucine (see Table 4). An affinity similar to that for the L1R substitution was observed for the methionine substitution (L1M). Since methionine is a smaller residue than arginine and on the other hand the lysine substitution (L1K) leads to a larger reduction in the affinity of the peptide than the L1R substitution, it is likely that a combination of size-dependent hydrophobic and electrostatic interactions involving the first residue of this peptide is important for binding to the channel. Taken together, all these results are completely inconsistent with Leu1 being the hydrophobic partner in a dyad. Interestingly, the dyad hypothesis is challenged in a recent publication by Mouhat et al. (*33*), who showed that the K24−Y33 functional dyad of the scorpion toxin Pi1 is not indispensable for recognition and binding to the voltage-gated $K_v1.2$ potassium channel. This conclusion, drawn from the observation of a partial but specific current reduction after application of the mutant [A24,A33]-Pi1, lacking the functional dyad, confirms our results and opens the way to considering different possible mechanisms for the interaction of toxins with K^+ channels.

κM-RIIIK, the Na^+ channel blocker μ-GIIIA, and the noncompetitive antagonist of nicotinic acetylcholine receptors ψ-PIIIF all share a common class III Cys pattern. The structural features of the three peptides are very similar toward the C-terminus, where all three conotoxins are folded in two distorted helical turns (Figure 3). However, toward the N-terminus, the three peptides show substantial differences in both structure and dynamics. While μ-GIIIA and ψ-PIIIF have a well-defined backbone folded in a series of turns, κM-RIIIK is highly flexible in the region of residues 1−11. It should be emphasized that the flexibility of the peptide is not an artifact due to poor structural restraints but an intrinsic dynamic feature of the molecule, as confirmed by the averaged values of the $^3J(H_N,H_\alpha)$ couplings, the small values of the $N-H_N$ dipolar couplings, and the higher values of the heteronuclear $^{13}C-^1H$ NOEs in this region. We suggest that the differences in the three-dimensional form, provided by the structural heterogeneity at the N-terminus, and in the surface charge distribution are an important determinant of target selectivity.

The localization of the functionally critical amino acids on the three-dimensional structure of κM-RIIIK is shown in Figure 6. The four most important residues (Leu1, Arg10, Lys18, and Arg19) and the seven residues of medium

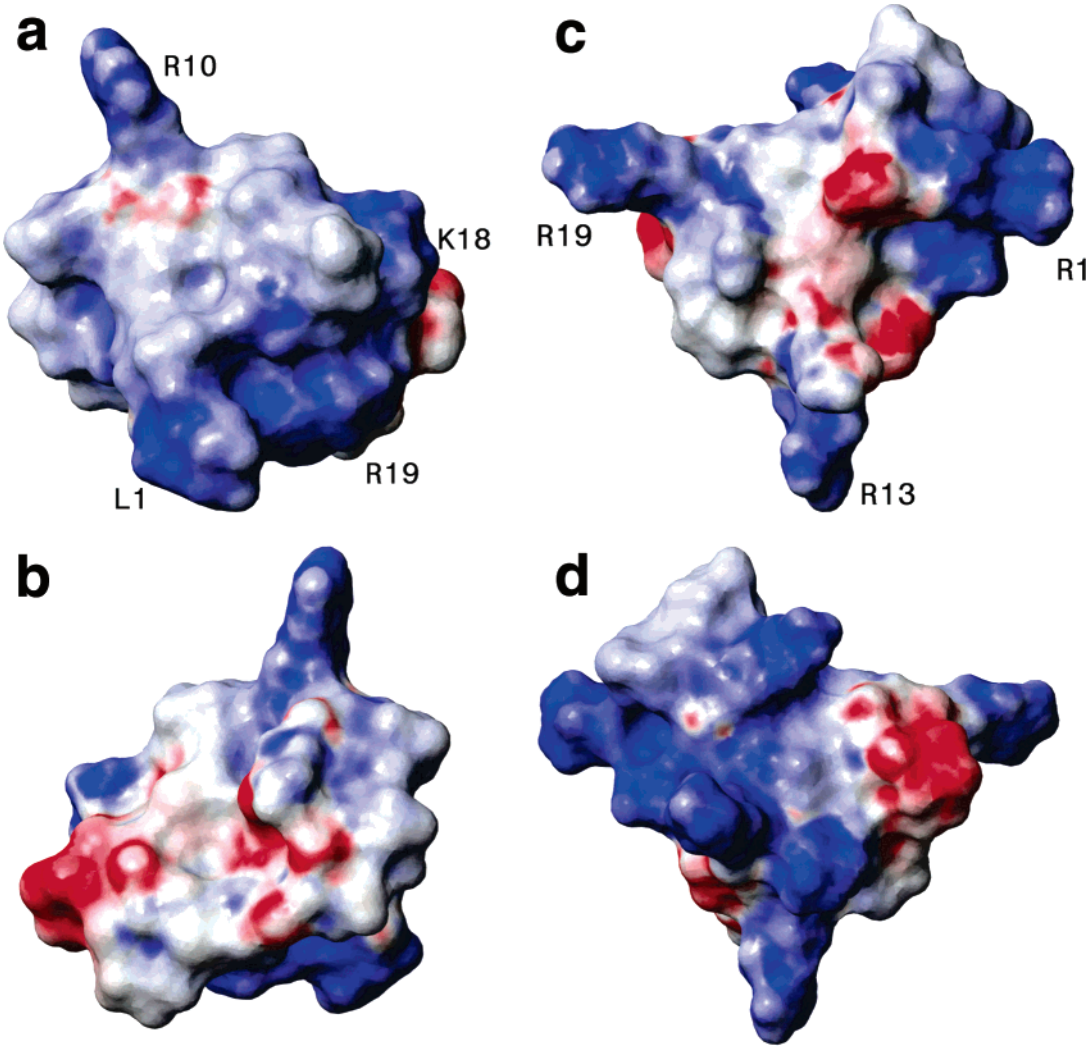

FIGURE 7: Electrostatic surface potential for κM-conotoxin RIIIK (a and b) and μ-contoxin GIIIA (c and d). The orientation of κM-conotoxin RIIIK is the same as in Figure 6. Intense blue and red regions correspond to charges of 1.0 and −1.0 or greater, respectively. The surface potential was calculated with the AvgCharge algorithm of MOLMOL 2k·2.

importance are distributed well across the whole molecule, as opposed to the commonly found structural motif for K^+ channel blockers that contains a dyad of a positively charged residue and a hydrophobic residue. The separation of key residues in κM-RIIIK resembles μ-GIIIA more than other K^+ channel-targeted toxins. However, all functionally relevant residues can be localized on a surface of 12 Å × 9 Å (Figure 6a), with the most important residues (in red) being situated at the edges and the residues of medium relevance (in yellow) in the middle of the surface. On the opposite side of the peptide (Figure 6b), no residue seems to be essential for function.

The charge distributions on the surfaces of κM-RIIIK, μ-GIIIA, and κ-PVIIA are substantially different. In κM-RIIIK, most of the positive charges are distributed at the edges of the peptide face containing the functionally essential amino acids (Figure 7a). It is noteworthy that in κM-RIIIK all determinants for binding contain a positive charge, and that all positively charged residues are necessary for binding. This ring of positive charges could be used as an anchor for residues of the K^+ channel loops. In μ-GIIIA and κ-PVIIA, the distribution of both charges and binding determinant residues on the peptide surface is more homogeneous than in κM-RIIIK. In μ-GIIIA, however, a ring of positive charges could be similarly identified at the height of R19 and R1 (Figure 7c,d). In contrast to the case for κM-RIIIK, a functionally highly relevant residue in μ-GIIIA, R13, sticks out from the surface defined by this ring and is probably projected into the channel pore. In κM-RIIIK, no additional positively charged residue sticks out from the surface defined by the ring of positively charged residues Leu1, Arg10, Lys18, and Arg19. This observation, together with the fact that κM-conotoxin RIIIK lacks a functional dyad, does not support the model of a positively charged side chain occluding the channel pore. On the contrary, the even distribution of Leu1, Arg10, Lys18, and Arg19 at the edges of the peptide face containing all functionally relevant residues suggests that conotoxin κM-RIIIK may block the channel by covering the pore as a lid. This pharmacophore model represents a novel mechanism of K^+ channel block that has not been found in any other K^+ channel-targeted peptide characterized to date. The recent paper by Mouhat et al. (*33*) demonstates the presence of a basic ring in scorpion toxin Pi1 that might be similar to the one described here, indicating that a similar pharmacophore has been independently evolved by cone snails and scorpions. Mutation and docking data reveal the importance of a cooperative electrostatic interaction of the basic residues of this ring in

scorpion toxin Pi1 with side chains of the turret region of the channel. These results reinforce our proposition of a different model of peptide−channel interaction that is not centered on a functional dyad. In a recent review of the interaction of several biodiverse scorpion toxins to K^+ channels (*34*), three different binding modes have been proposed: internal mode, involving residues at the turret region, the pore helix, and the selectivity filter of the channel; intermediate mode, involving residues at the turret region and the bottom of the vestibule of the channel; and external mode, involving residues that are distant from the channel selectivity filter. This idea is supported by the observation that scorpion toxin BmTx3 can block A-type K^+ and Herg currents using two different faces (*35*), suggesting the existence of two different binding modes (*36*). The pharmacophore model that we propose for the interaction of κM-conotoxin RIIIK with the *TSha1* K^+ channel most likely resembles the intermediate binding mode.

The structure−function study reported here is broadly significant because κM-RIIIK is at the unique intersection between structural similarity and similar target specificity. We have provided direct evidence that κM-conotoxin RIIIK and κ-conotoxin PVIIA, which both inhibit the same K^+ channel subtypes, are both structurally divergent and mechanistically dissimilar. In contrast, κM-conotoxin RIIIK is structurally highly similar to genetically related conotoxins (i.e., μ-conotoxin GIIIA and ψ-conotoxin PIIIF), which have a completely different target specificity (K^+ channels, Na^+ channels, and Ach receptors). This provides a potential framework for understanding both molecular convergence and divergence in ion channel-targeted ligands.

ACKNOWLEDGMENT

We thank Dr. R. J. French and Dr. C. Griesinger for helpful discussions during this project. The technical assistance of Mona Honemann and Nina Strüver is greatly appreciated. We thank L. Cervini for the identification of the Cys5−Cys22 disulfide bridge, W. Low for mass spectrometric analysis, and D. Kirby and C. Miller for HPLC and CZE analyses.

REFERENCES

1. Miller, C. (1995) The charybdotoxin family of K^+ channel-blocking peptides, *Neuron 15*, 5−10.
2. Eriksson, M. A. L., and Roux, B. (2002) Modeling the structure of agitoxin in complex with the *Shaker* K^+ channel: a computational approach based on experimental distance restraints extracted from thermodynamic mutant cycles, *Biophys. J. 83*, 2595−2609.
3. Gao, Y.-D., and Garcia, M. (2003) Interaction of agitoxin2, charybdotoxin, and iberiotoxin with potassium channels: Selectivity between voltage-gated and Maxi-K channels, *Proteins 52*, 146−154.
4. Stampe, P., Kolmakovapartensky, L., and Miller, C. (1994) Intimations of K^+ channel structure from a complete functional map of the molecular-surface of charybdotoxin, *Biochemistry 33*, 443−450.
5. Dauplais, M., Lecoq, A., Song, J., Cotton, J., Jamin, N., Gilquin, B., Roumestand, C., Vita, C., de Medeiros, C. L. C., Rowan, E., Harvey, A. L., and Ménez, A. (1997) On the convergent evolution of animal toxins, *J. Biol. Chem. 272*, 4302−4309.
6. Savarin, P., Guenneugues, M., Gilquin, B., Lamthanh, H., Gasparini, S., Zinn-Justin, S., and Ménez, A. (1998) Three-dimensional structure of κ-conotoxin PVIIA, a novel potassium channel-blocking toxin from cone snails, *Biochemistry 37*, 5407−5416.
7. Gilquin, B., Racapé, J., Wrisch, A., Visan, V., Lecoq, A., Grissmer, S., Ménez, A., and Gasparini, S. (2002) Structure of the BgK−Kv1.1 complex based on distance restraints identified by double mutant cycles, *J. Biol. Chem. 277*, 37406−37413.
8. Srinivasan, K. N., Sivaraja, V., Huys, I., Sasaki, T., Cheng, B., Kumar, T. K. S., Sato, K., Tytgat, J., Yu, C., Ching San, B. C., Ranganathan, S., Bowie, J. H., Kini, R. M., and Gopalakrishnakone, P. (2002) κ-Hefutoxin1, a novel toxin from the scorpion *Heterometrus fulvipes* with unique structure and function: importance of the functional diad in potassium channel selectivity, *J. Biol. Chem. 277*, 30040−30047.
9. Rauer, H., Pennington, M., Cahalan, M., and Chandy, K. G. (1999) Structural conservation of the pores of calcium-activated and voltage-gated potassium channels determined by a sea anemone toxin, *J. Biol. Chem. 274*, 21885−21892.
10. Jacobson, R. B. E., Koch, D., Lange-Malecki, B., Stocker, M., Verhey, J., Van Wagoner, R. M., Vyazovkina, A., Olivera, B. M., and Terlau, H. (2000) Single amino acid substitutions in κ-conotoxin PVIIA disrupt interaction with the *Shaker* channel, *J. Biol. Chem. 275*, 24639−24644.
11. Terlau, H., and Olivera, B. M. (2004) *Conus* venoms: A rich source of novel ion channel-targeted peptides, *Physiol. Rev. 84*, 41−68.
12. Terlau, H., Shon, K. J., Grilley, M., Stocker, M., Stühmer, W., and Olivera, B. M. (1996) Strategy for rapid immobilization of prey by a fish-hunting marine snail, *Nature 381*, 148−151.
13. Shon, K., Stocker, M., Terlau, H., Stühmer, W., Jacobsen, R., Walker, C., Grilley, M., Watkins, M., Hillyard, D. R., Gray, W. R., and Olivera, B. M. (1998) κ-Conotoxin PVIIA: a peptide inhibiting the *Shaker* K^+ channel, *J. Biol. Chem. 273*, 33−38.
14. Ferber, M., Sporning, A., Jeserich, G., Cruz, R., Watkins, M., Olivera, B. M., and Terlau, H. (2003) A novel *Conus* peptide ligand for K^+ channels, *J. Biol. Chem. 278*, 2177−2183.
15. Stewart, J., Pèna, C., Matsueda, G. R., and Haris, K. (1976) Some improvements in the solid phase synthesis of large peptides, *The 14th European Peptide Symposium*, pp 285−290, Editions de l'Université de Bruxelles, Bruxelles (Belgique), Wépion, Belgium.
16. Kaiser, E., Colescott, R. L., Bossinger, C. D., and Cook, P. I. (1970) Color test for detection of free terminal amino groups in the solid-phase synthesis of peptides, *Anal. Biochem. 34*, 595−598.
17. Miller, C., and Rivier, J. (1996) Peptide chemistry: Development of high-performance liquid chromatography and capillary zone electrophoresis. *Biopolymers 40*, 265−317.
18. Miller, C., and Rivier, J. (1998) Analysis of synthetic peptides by capillary zone electrophoresis in organic/aqueous buffers, *J. Pept. Res. 51*, 444−451.
19. Rückert, M., and Otting, G. (2000) Alignment of biological macromolecules in novel nonionic liquid crystalline media for NMR experiments, *J. Am. Chem. Soc. 122*, 7793−7797.
20. Wüthrich, K. (1986) *NMR of proteins and nucleic acids*, Wiley, New York.
21. Jeener, J., Meier, B. H., Bachmann, P., and Ernst, R. R. (1979) Investigation of exchange processes by 2-dimensional NMR spectroscopy, *J. Chem. Phys. 71*, 4546−4553.
22. Rance, M., Sørensen, O. W., Bodenhausen, G., Wagner, G., Ernst, R. R., and Wüthrich, K. (1983) Improved spectral resolution in COSY ^{1}H-NMR spectra of proteins via double quantum filtering, *Biochem. Biophys. Res. Commun. 117*, 479−485.
23. Braunschweiler, L., and Ernst, R. R. (1983) Coherence transfer by isotropic mixing: Application to proton correlation spectroscopy. *J. Magn. Reson. 53*, 521−528.
24. Bax, A., Ikura, M., Kay, L. E., Torchia, D. A., and Tschudin, R. (1990) Comparison of different modes of 2-dimensional reverse-correlation NMR for the study of proteins. *J. Magn. Reson. 86*, 304−318.
25. Brünger, A. T. (1993) *X-PLOR Version 3.1: A system for X-ray crystallography and NMR*, Yale University Press, New Haven, CT.
26. Krieg, P. A., and Melton, D. A. (1987) *In vitro* RNA-synthesis with SP6 RNA-polymerase, *Methods Enzymol. 155*, 397−415.
27. Hill, J. M., Alewood, P. F., and Craik, D. J. (1996) Three-dimensional solution structure of μ-conotoxin GIIIB, a specific blocker of skeletal muscle sodium channels. *Biochemistry 35*, 8824−8835.

28. Lancelin, J. M., Kohda, S., Tate, Y., Yanagawa, T., Satake, A. M., and Inagaki, F. (1991) Tertiary structure of conotoxin GIIIA in aqueous-solution, *Biochemistry 30*, 6908−6916.
29. Wakamatsu, K., Kohda, D., Hatanaka, H., Lancelin, J. M., Ishida, Y., Oya, M., Nakamura, H., Inagaki, F., and Sato, K. (1992) Structure−activity relationships of m-conotoxin GIIIA: structure determination of active and inactive sodium-channel blocker peptides by NMR and simulated annealing calculations, *Biochemistry 31*, 12577−12584.
30. Van Wagoner, R. M., Jacobsen, R. B., Olivera, B. M., and Ireland, C. M. (2003) Characterization and three-dimensional structure determination of ψ-conotoxin PIIIF, a novel noncompetitive antagonist of nicotinic acetylcholine receptors, *Biochemistry 42*, 6353−6362.
31. Van Wagoner, R. M., and Ireland, C. M. (2003) An improved solution structure for y-conotoxin PIIIE, *Biochemistry 42*, 6347−6352.
32. Rivier, J. E., Hoeger, C., Erchegyi, J., Gulyas, J., DeBoard, R., Craig, A. G., Koerber, S. C., Wenger, S., Waser, B., Schaer, J.-C., and Reubi, J. C. (2001) Potent somatostatin undecapeptide agonists selective for somatostatin receptor 1 (sst1), *J. Med. Chem. 44*, 2238−2246.
33. Mouhat, S., Mosbah, A., Visan, V., Wulff, H., Delepierre, M., Darbon, H., Grissmer, S., De Waard, M., and Sabatier, J.-M. (2004) The functional dyad of scorpion toxin Pi1 is not itself a prerequisite for toxin binding to the voltage-gated Kv1.2 potassium channels, *Biochem. J. 377*, 25−36.
34. Rodriguez de la Vega, R. C., Merino, E., Becerril, B., and Possani, L. D. (2003) Novel interactions between K^+ channels and scorpion toxins, *Trends Pharmacol. Sci. 24*, 222−227.
35. Huys, I., Xu, C.-Q., Wang, C.-Z., Vacher, H., Martin-Eauclaire, M.-F., Chi, C.-W., and Tytgat, J. (2004) Bm Tx3, a scorpion toxin with two putative functional faces separately active on A-type K^+ and Herg currents, *Biochem. J. 378*, 745−752.
36. Xu, C.-Q., Zhu, S.-Y., Chi, C.-W., and Tytgat, J. (2003) Turret and pore block of K^+ channels: what is the difference? *Trends Pharmacol. Sci. 24*, 446−448.

BI0495681